

Neuronal Excitability

Context-Dependent Modulation of Excitatory Synaptic Strength by Synaptically Released Zinc

Bopanna I. Kalappa and  Thanos TzounopoulosDOI:<http://dx.doi.org/10.1523/ENEURO.0011-17.2017>

Departments of Otolaryngology and Neurobiology, University of Pittsburgh, Pittsburgh, PA 15261

Abstract

Synaptically released zinc inhibits baseline excitatory neurotransmission; however, the role of this neuromodulator on short-term plasticity during different levels of synaptic activity remains largely unknown. This lack of knowledge prevents our understanding of information transfer across zinc-releasing synapses, including 50% of excitatory synapses in cortical areas. We used *in vitro* electrophysiology in mouse brain slices and discovered that the effects of zinc on excitatory postsynaptic current (EPSC) amplitudes are context-dependent. At lower frequencies of activity, synaptically released zinc reduces EPSC amplitudes. In contrast, at higher stimulation frequencies and vesicular release probability (Pr), zinc inhibits EPSC amplitudes during the first few stimuli but leads to enhanced steady-state EPSC amplitudes during subsequent stimuli. This paradoxical enhancement is due to zinc-dependent potentiation of synaptic facilitation via the recruitment of endocannabinoid signaling. Together, these findings demonstrate that synaptically released zinc is a modulator of excitatory short-term plasticity, which shapes information transfer among excitatory synapses.

Key words: auditory brainstem; auditory synapses; short-term plasticity; synaptic zinc; ZnT3

Significance Statement

In many brain areas, including the neocortex, limbic structures, and auditory brainstem, glutamatergic nerve terminals contain zinc in their synaptic vesicles. Zinc is loaded into these vesicles by zinc transporter 3 and is coreleased with glutamate. Synaptically released zinc is an inhibitory neuromodulator in excitatory synapses, but the role of zinc in short-term plasticity remains unknown. Our results suggest that zinc shapes excitatory synaptic strength in a manner dependent on frequency and activity level. Namely, during low vesicular release probability (Pr) and low-frequency stimulation, zinc inhibits EPSCs; during higher Pr and prolonged presynaptic stimulation, zinc enhances steady-state EPSCs.

Introduction

Zinc is an essential element for cellular function. Divalent zinc is a cofactor in a large number of enzymes and regulatory proteins (Vallee, 1988), and as such, the chemistry and biology of zinc metalloproteins have historically dominated the field of zinc biology. However, in recent years there has been growing evidence for a signaling role of mobile chelatable zinc, which is released in tissues such as the prostate, pancreas, and brain (Frederickson et al., 2005; Kelleher et al., 2011). In the brain, the vesic-

ular zinc transporter, ZnT3, sequesters zinc into synaptic glutamatergic vesicles in many excitatory synapses. In the cortex, more than 50% of excitatory presynaptic terminals have vesicles that contain ZnT3, attesting to zinc's importance in synaptic transmission (Sindreu et al., 2003; Frederickson et al., 2005). Recent studies used novel tools for chelating and tracking zinc in central synapses and established that zinc is a phasically released inhibitory neuromodulator in excitatory synapses. In response to a single presynaptic action potential, synaptic zinc is re-

Received January 10, 2017; accepted February 9, 2017; First published February 15, 2017.

Authors report no conflict of interest.

Author contributions: BIK performed research; BIK and TT analyzed data; BIK and TT wrote the paper.

This work was supported by National Institutes of Health grants DC007905

leased from the presynaptic terminal and inhibits postsynaptic glutamate AMPA and NMDA receptor EPSCs (NMDARs/AMPA) via postsynaptic mechanisms (Pan et al., 2011; Kalappa et al., 2015). Moreover, during brief repetitive synaptic stimulation, zinc inhibits synaptic and extrasynaptic glutamate NMDARs via postsynaptic mechanisms (Vergnano et al., 2014; Anderson et al., 2015) and is necessary—along with GPR39, a putative metabotropic zinc-sensing receptor—for activation of endocannabinoid signaling and inhibition of vesicular release probability (Pr; Perez-Rosello et al., 2013).

Zinc is released from glutamatergic vesicles and inhibits excitatory synaptic strength via pre- and postsynaptic mechanisms. Therefore, it is essential to study the mechanisms and dynamics of zinc modulation of excitatory neurotransmission during ongoing synaptic activity. The determination of these mechanisms will be crucial for understanding the role of synaptically released zinc in information transfer among excitatory synapses during different levels of synaptic activity. To study this issue, we combined electrophysiological, pharmacological, and genetic techniques.

Materials and Methods

Animals

In this study, we used male or female ICR mice (Harlan Laboratory) and ZnT3 wild-type (WT) and knockout (KO) littermate mice (Jackson Laboratory) aged from postnatal day 18 (P18) to P28. All animal procedures were approved by the Institutional Animal Care and Use Committee of the University of Pittsburgh, Pittsburgh, PA.

Electrophysiology

Brain slice preparation and electrophysiological experiments were carried out using extracellular solution artificial cerebrospinal fluid (ACSF) of the following composition (in mM): 130 NaCl, 3 KCl, 1.2 CaCl₂·2H₂O, 1.8 MgCl₂·6H₂O, 20 NaHCO₃, 3 HEPES, and 10 D-glucose, saturated with 95% O₂/5% CO₂ (vol/vol), pH 7.25–7.35, ~300 mOsm. To minimize changes in excitability of parallel fibers when switching ACSFs, divalent ion concentrations were optimized as follows: 1.2 mM external calcium ACSF consisted of 1.2 mM CaCl₂ and 1.8 mM MgCl₂, and 2.4 mM external calcium ACSF consisted of 2.4 mM CaCl₂ and 0.6 mM MgCl₂. Contaminating zinc was removed from the ACSF by stirring the ACSF with Chelex 100 resin (Bio-Rad) for 1 h. High-purity CaCl₂·2H₂O and MgCl₂·6H₂O salts (99.995% purity; Sigma-Aldrich) were added to the ACSF after the Chelex resin was filtered

using Nalgene rapid-flow filters lined with polyethersulfone (0.2- μ m pore size). All plastic and glassware used in these experiments were washed with 5% high-purity nitric acid. For brain slice preparations, mice were first anesthetized with isoflurane (3%) and then immediately decapitated. Brains were rapidly removed, and coronal slices (210 μ m) of the left dorsal cochlear nucleus (DCN) were prepared in 1.2 mM external calcium containing ACSF at 35°C using a Vibratome (VT1200 S; Leica). Slices were then transferred to a holding chamber, where they were incubated for ~60 min at 35°C. After incubation, slices were maintained at room temperature and used for experiments up to a duration of 4 h. For electrophysiological experiments, slices were transferred into the recording chamber and perfused with ACSF at a rate of 1–2 ml/min. Cartwheel cells in the molecular layer of the DCN were identified by their characteristic firing pattern that consists of simple and complex spikes (Zhang and Oertel, 1993; Manis et al., 1994; Tzounopoulos et al., 2004). Electrophysiological recordings were made using a MultiClamp-700B amplifier equipped with Digidata-1440A A/D converter (Molecular Devices). Whole-cell voltage-clamp recordings were conducted at –40 mV holding potential, except for Figs. 1 and 6, where neurons were held at –70 mV. For whole-cell recordings, we used borosilicate fire-polished glass pipettes with filament (Sutter Instruments). Recording pipettes were filled with a cesium-based internal solution with the following composition (in mM): 126 CsCH₃O₃S, 4 KCl, 10 HEPES, 4 Na₂ATP, 0.3 Tris-GTP, 10 Tris-phosphocreatine, 1 Cs₂EGTA, 1 QX-314, and 3 sodium ascorbate (pH 7.25, 295 mOsm), 3–5 M Ω resistance. Experimental results reported in Figs. 1 and 6 were conducted using a K-based internal solution containing (in mM) 113 K-gluconate, 4.5 MgCl₂·6H₂O, 14 Tris-phosphocreatine, 9 HEPES, 0.1 EGTA, 4 Na₂ATP, 0.3 Tris-GTP, and 10 sucrose (pH 7.3, 300 mOsm). Recordings were conducted at 34–37°C using an inline heating system. Electrode series resistance was compensated at 70%–80% on-line using a 10- μ s lag. Data were sampled at 10 or 20 kHz and filtered at 4 or 8 kHz. AMPA EPSCs in cartwheel cells were evoked by stimulating parallel fibers with an Isoflex stimulator (AMPI) using ACSF containing glass theta electrodes. AMPA EPSC peak amplitudes were measured from the baseline obtained by extrapolating the decay of the preceding AMPA EPSC using a single-exponential function. All experiments were conducted in the presence of glycine and GABA_A receptor blockers, strychnine (1 μ M), and SR95531 (20 μ M), respectively. To validate that NMDARs do not contribute to the zinc-mediated effects during the train, experiments in Fig. 2 and Fig. 3 were conducted in the presence of 50 μ M of NMDAR antagonist, DL-APV. ZX1 (100 μ M), AM-251 (1 μ M), WIN 55, 212-2 (50 nM), cyclothiazide (100 μ M), and kynurenic acid (0.5–1 mM) were always bath applied. All drugs were dissolved in deionized water, except for WIN 55, 212-2, which used DMSO as vehicle; the final concentration of DMSO was <0.5%. The experimenter was blinded to the genotype in experiments involving ZnT3WT and ZnT3KO mice. Once the experimenter completed the analysis of experiments from individual mice, he received

(TT) and T32DC011499 (BIK).

Acknowledgments: We thank Dr. Elias Aizenman for helpful discussions and critical reading of the manuscript.

Correspondence should be addressed to Thanos Tzounopoulos, Department of Otolaryngology, University of Pittsburgh, Biomedical Science Tower 3, Room 3017, 3501 Fifth Avenue, Pittsburgh, PA 15261. E-mail: thanos@pitt.edu.

DOI: <http://dx.doi.org/10.1523/ENEURO.0011-17.2017>

Copyright © 2017 Kalappa and Tzounopoulos

This is an open-access article distributed under the terms of the Creative Commons Attribution 4.0 International, which permits unrestricted use, distribution and reproduction in any medium provided that the original work is properly attributed.

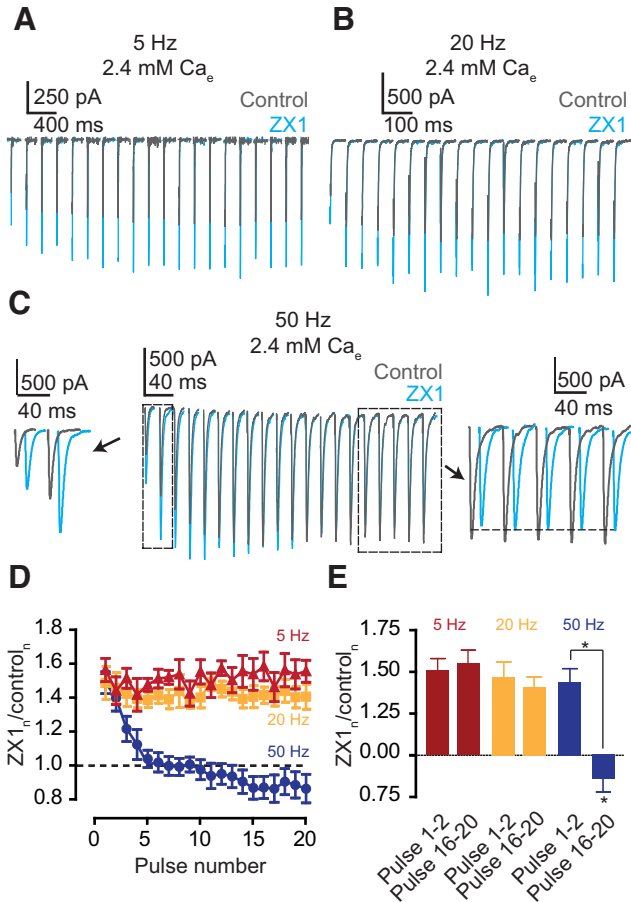


Figure 1. Frequency- and history-dependent effects of synaptically released zinc on AMPA EPSCs. **A–C**, Representative traces of cartwheel cell AMPA EPSCs evoked by 20-pulse train stimulation of parallel fiber at 5 Hz (**A**), 20 Hz (**B**), and 50 Hz (**C** middle panel), before (grey) and after 100 μ M ZX1 (blue); (**C** side panels) same as in upper panel but zoomed on the first 2 pulses (left) and the last 5 pulses (right). For improved visualization, responses after ZX1 are slightly shifted to the right. **D**, Summary graph showing the ratio of AMPA EPSCs in ZX1 to that in control at each pulse at 5 Hz (maroon), 20 Hz (orange), and 50 Hz (blue). **E**, Summary graph comparing the ratio of AMPA EPSCs in ZX1 to that in control for the first two and last five pulses in the 20-pulse train at 5 Hz (maroon, $n = 10$, $p = 0.82$), 20 Hz (orange, $n = 10$, $p = 0.63$), and 50 Hz (blue, $n = 10$, $p < 0.01$). Values represent mean \pm SEM. Detailed values and statistical tests: **D**, **E**, $ZX1_{1-2}/control_{1-2}$ vs. $ZX1_{16-20}/control_{16-20}$: 5 Hz: 1.51 ± 0.07 vs. 1.55 ± 0.08 , $n = 10$, $p = 0.82$, $t = 0.24$, $df = 9$; 20 Hz: 1.47 ± 0.09 vs. 1.41 ± 0.06 , $n = 10$, $p = 0.63$, $t = 0.49$, $df = 9$; 50 Hz: 1.44 ± 0.07 vs. 0.86 ± 0.08 , $n = 10$, $p < 0.01$, $t = 5.45$, $df = 9$; paired t -tests; $ZX1_{1-2}/control_{1-2}$: 5 Hz vs. 20 Hz, $p = 0.65$, $t = 0.46$, $df = 9$; 5 Hz vs. 50 Hz, $p = 0.38$, $t = 0.92$, $df = 9$; 20 Hz vs. 50 Hz, $p = 0.68$, $t = 0.42$, $df = 9$; $ZX1_{16-20}/control_{16-20}$: 5 Hz vs. 20 Hz, $p = 0.09$, $t = 1.87$, $df = 9$; 5 Hz vs. 50 Hz, $p < 0.01$, $t = 5.09$, $df = 9$; 20 Hz vs. 50 Hz, $p < 0.01$, $t = 4.98$, $df = 9$; paired t -tests; AMPA EPSC amplitudes $_{16-20}$: control: 50 Hz: 1.00 ± 0.00 vs. ZX1: 0.86 ± 0.08 , $p = 0.042$, $t = 2.36$, $df = 9$; one-sample t -test.

information regarding the grouping of mice. After the experimenter averaged the data from the two groups of mice, he was informed on the genotype of the two groups.

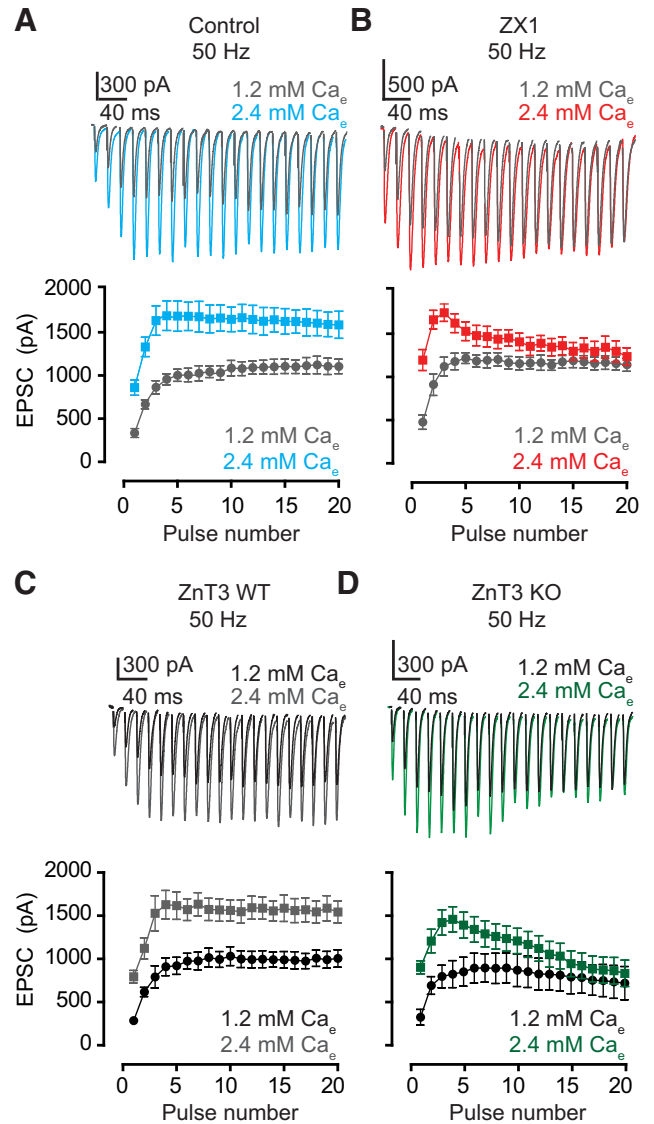


Figure 2. ZnT3-dependent, synaptically released zinc enhances EPSC_{SS} in high Pr. **A**, **B**, Upper panels, representative traces of AMPA EPSCs evoked by 50-Hz 20-pulse train in 1.2 mM (gray) and 2.4 mM (color) external calcium in control (**A**) and ZX1 (**B**). Lower panels, summary graphs showing average AMPA EPSC amplitudes during the train in 1.2 mM (gray) and 2.4 mM (color) external calcium in control (**A**) and ZX1 (**B**); EPSC₁₆₋₂₀ amplitude: control: 1.2 vs. 2.4 mM: $n = 7$, $p < 0.01$; ZX1: 1.2 vs. 2.4 mM: $n = 7$, $p = 0.09$). **C**, **D**, Upper panels, representative traces of AMPA EPSCs evoked by 50-Hz 20-pulse train in 1.2 mM (black) and 2.4 mM (gray or green) external calcium in ZnT3WT (**C**) and ZnT3KO mice (**D**). Lower panels, summary graphs showing average AMPA EPSC amplitudes during the train in 1.2 mM (black) and 2.4 mM (gray or green) external calcium in ZnT3WT (**C**) and ZnT3KO mice (**D**); ZnT3 WT: 1.2 vs. 2.4 mM: $n = 5$, $p < 0.01$; ZnT3KO: 1.2 vs. 2.4 mM: $n = 5$, $p = 0.24$). Values represent mean \pm SEM.

Detailed values and statistical tests. **A**, **B**, lower panels: EPSC₁₆₋₂₀ amplitude: control: 1.2 mM calcium: $1109 \text{ pA} \pm 90 \text{ pA}$ vs. 2.4 mM calcium: $1605 \text{ pA} \pm 147 \text{ pA}$, $n = 7$, $p < 0.01$, $F = 40.89$, $DFn = 1$, $DFd = 60$; ZX1: 1.2 mM calcium: $1158 \text{ pA} \pm 75 \text{ pA}$ vs. 2.4 mM calcium: $1301 \text{ pA} \pm 116 \text{ pA}$, $n = 7$, $p = 0.09$, $F = 2.9$, $DFn = 1$, $DFd = 60$; two-way ANOVA. **C**, **D**, lower panels:

continued

EPSC_{16–20} amplitude. ZnT3WT: 1.2 mM calcium: 996 pA ± 95 pA vs. 2.4 mM calcium: 1564 pA ± 135 pA, $n = 5$, $p < 0.01$, $F = 58.51$, $DFn = 1$, $DFd = 40$; ZnT3KO: 1.2 mM calcium: 750 pA ± 185 pA vs. 2.4 mM calcium: 876 pA ± 156 pA, $n = 5$, $p = 0.24$, $F = 1.40$, $DFn = 1$, $DFd = 40$; two-way ANOVA.

Drugs

SR95531, DL-APV, and strychnine were purchased from Hello-Bio. AM-251, WIN 55, 212-2, QX-314, cyclothiazide, and kynurenic acid were purchased from Tocris. ZX1 was purchased from STREM Chemicals.

Statistics

For statistical comparisons, paired t tests and unpaired t tests were used if the group data passed the Lilliefors test for normality. If the group data were not normally distributed, then the Wilcoxon rank sum test was used. For normalized data, one-sample t -test was used. We used two-way ANOVA for comparisons of data groups

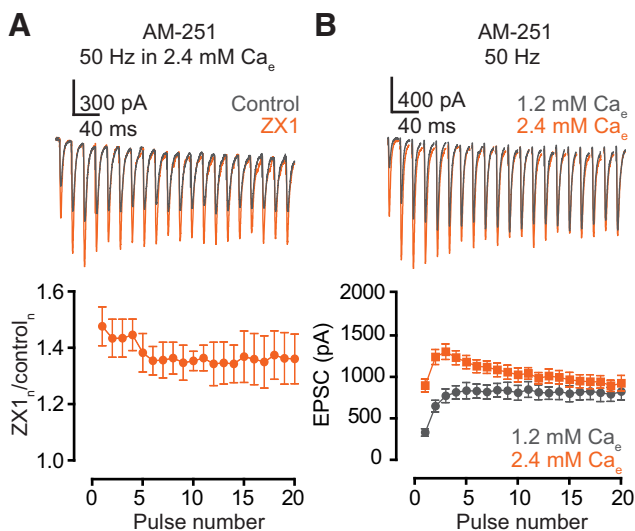


Figure 3. Endocannabinoid signaling is necessary for the zinc-mediated enhancement of EPSC_{SS}. **A**, Upper panel, representative traces of AMPA EPSCs, evoked by 50-Hz 20-pulse train, in the presence of 1 μ M AM-251 before (gray) and after ZX1 (orange). Lower panel, summary graph showing average ratios of AMPA EPSCs in the presence of ZX1 to that in control during the train ($ZX_{1-2}/control_{1-2}$ vs. $ZX_{16-20}/control_{16-20}$; 50 Hz: $n = 5$, $p = 0.13$). **B**, Upper panel, representative traces of AMPA EPSCs evoked by 50-Hz 20-pulse train in 1.2 mM (gray) and 2.4 mM (orange) external calcium in the presence of AM-251. Lower panel, summary graph showing average AMPA EPSC amplitudes during the train in 1.2 mM (gray) and 2.4 mM (orange) external calcium in the presence of AM-251. (EPSC_{16–20} amplitude in AM-251: 1.2 vs. 2.4 mM calcium, $n = 5$, $p = 0.09$). Values represent mean ± SEM.

Detailed values and statistical tests: **A**, lower panel: $ZX_{1-2}/control_{1-2}$ vs. $ZX_{16-20}/control_{16-20}$; 50 Hz: control: 1.47 ± 0.06 vs. ZX1: 1.36 ± 0.08 , $n = 5$, $p = 0.13$, $t = 1.4$, $df = 9$; paired t -test. **B**, lower panel: EPSC_{16–20} amplitude: AM-251: 1.2 mM calcium: $805 \text{ pA} \pm 97 \text{ pA}$ vs. 2.4 mM calcium: $921 \text{ pA} \pm 80 \text{ pA}$, $n = 5$, $p = 0.19$, $F = 1.7$, $DFn = 1$, $DFd = 40$; two-way ANOVA.

including multiple Ca levels shown in Figs. 2, 3B, 4B, 4D, 5A, 5B, 6A, 6G, and 7B.

Results

Synaptically released zinc enhances steady-state AMPA EPSC during high Pr and high-frequency trains

To investigate the impact of synaptically released zinc in neurotransmission during different frequencies and levels of synaptic activity, we studied zinc-mediated neuromodulation in cartwheel cells. Cartwheel cells represent a class of inhibitory interneurons located in the molecular layer of the DCN, a cerebellar-like structure in the auditory brainstem (Oertel and Young, 2004). Cartwheel cells receive glutamatergic input from zinc-rich parallel fibers (PFs; Frederickson et al., 1988). In response to PF stimulation by a 20-pulse train at 5 or 20 Hz, zinc chelation with the extracellular, high-affinity, fast chelator, ZX1 (Pan et al., 2011; Anderson et al., 2015), potentiated AMPA EPSC amplitudes (Fig. 1A, B). Moreover, the amount of this increase was constant throughout the stimulus train (Fig. 1A, B, D, E). This result suggests that the effect of zinc is a steady subtractive inhibition of AMPA EPSC, readily predicted by the postsynaptic inhibitory effect of zinc on AMPARs in response to a single stimulus (Kalappa et al., 2015). In contrast to these findings, during the 20-pulse stimulation at 50 Hz, ZX1 enhanced AMPA EPSC in the first two to four pulses but, paradoxically, inhibited steady-state responses (EPSC_{SS}) during the last four pulses (Fig. 1C–E). This result suggests that the modulatory effects of zinc depend on the history of the synapse: during high-frequency stimulation, zinc inhibits EPSCs for the first few stimuli, but later in the stimulus train, it enhances EPSC_{SS}. Given the known inhibitory role of zinc on synaptic strength, the zinc-mediated enhancement of EPSC_{SS} was unexpected.

The zinc-dependent enhancing effect on EPSC_{SS} was observed during high-frequency stimulation, which is associated with increases in Pr. To further interrogate the influence of Pr on EPSC_{SS} amplitudes, we manipulated Pr by using different extracellular calcium concentrations (Ca_e). Within the same cell, increasing Ca_e from 1.2 mM (low Pr) to 2.4 mM (high Pr) resulted in an increase in EPSC_{SS} amplitude (Fig. 2A). Previous studies on the homologous cerebellar PF synapses onto Purkinje neurons, which lack synaptic zinc, showed that alterations in Pr do not affect EPSC_{SS} amplitudes during 50-Hz trains (Kreitzer and Regehr, 2000). Because zinc enhances AMPA EPSC_{SS} in DCN synapses during high-frequency trains (Fig. 1C, E), we hypothesized that zinc signaling is necessary for the increase in steady-state responses in higher Ca_e. To test this hypothesis, we conducted similar experiments as in Fig. 2A but in the presence of ZX1. In these experiments, stimulation of PFs using the same 20-pulse 50-Hz train resulted in AMPAR EPSC_{SS} amplitudes that were not different between high and low Pr conditions (Fig. 2B). These results suggest that during high-frequency stimulation, endogenous zinc enhances EPSC_{SS} in higher Pr.

To determine whether synaptically released zinc was required for the enhanced EPSC_{SS} during high-frequency stimulation, we investigated EPSCs in PF to cartwheel cell synapses from mice lacking the ZnT3 transporter (ZnT3KO mice), which lack synaptically released zinc throughout the brain (Cole et al., 1999). In ZnT3KO mice, EPSC_{SS} evoked by a 20-pulse train stimulus at 50 Hz did not differ between 1.2 and 2.4 mM Ca_e (Fig. 2D), but EPSC_{SS} in ZnT3WT mice were larger in 2.4 mM Ca_e (Fig. 2C). Given that tonic zinc levels in the DCN are ZnT3 independent (Anderson et al., 2015), these results suggest that ZnT3-dependent synaptically released zinc enhances EPSC_{SS} in high Pr.

Synaptic zinc-mediated endocannabinoid signaling enhances steady-state AMPAR EPSC by enhancing synaptic facilitation

Zinc triggers endocannabinoid release after trains of presynaptic action potentials (Perez-Rosello et al., 2013). We therefore tested whether endocannabinoid signaling is necessary for the zinc-dependent enhancement of EPSC_{SS}. In the presence of 1 μM AM-251, a cannabinoid receptor 1 specific antagonist (Lan et al., 1999), we did not observe any change in the amount of ZX1 potentiation throughout the 50-Hz stimulation (Fig. 3A). Moreover, in ZX1, EPSC_{SS} were not different between 1.2 and 2.4 mM Ca_e (Fig. 3B). These results suggest that endocannabinoid signaling is necessary for the zinc-dependent enhancement of EPSC_{SS}.

By reducing Pr (Kreitzer and Regehr, 2002; Wilson and Nicoll, 2002), endocannabinoid signaling may also reduce the effect of postsynaptic factors that inhibit EPSC_{SS}, such as receptor saturation and desensitization (Trussell et al., 1993; Wadiche and Jahr, 2001; Chen et al., 2002; Foster et al., 2002). Alternatively, endocannabinoid signaling may enhance presynaptic factors that also enhance EPSC_{SS}, such as synaptic facilitation (Zucker and Regehr, 2002).

First we investigated whether reductions in AMPAR saturation or desensitization contribute to enhanced EPSC_{SS}. Namely, in ZX1, we measured the effect of kynurenic acid (0.5–1 mM) or cyclothiazide (100 μM) in EPSC_{SS}, with either 1.2 or 2.4 mM Ca_e. Kynurenic acid is a competitive AMPAR antagonist (Fig. 4A) that inhibits receptor saturation, and cyclothiazide is an allosteric modulator (Fig. 4C) that inhibits AMPAR desensitization (Partin et al., 1994, 1996; Neher and Sakaba, 2001; Prescott et al., 2006). If the enhancing effect of zinc on EPSC_{SS} was mediated by a zinc-driven decrease in AMPAR saturation or desensitization, blockade of these processes would enhance EPSC_{SS} in high Pr even in the presence of ZX1. Under these conditions, high Pr did not enhance EPSC_{SS} (Fig. 4B, D), suggesting that the enhancing effect of zinc on EPSC_{SS} is not due to either AMPAR saturation or desensitization.

Next we investigated whether endogenous zinc enhances EPSC_{SS} by endocannabinoid-mediated Pr reduction and a subsequent enhancement of synaptic facilitation. Consistent with this hypothesis, ZX1 decreased AMPA EPSC facilitation at 50 Hz (Fig. 5A). In

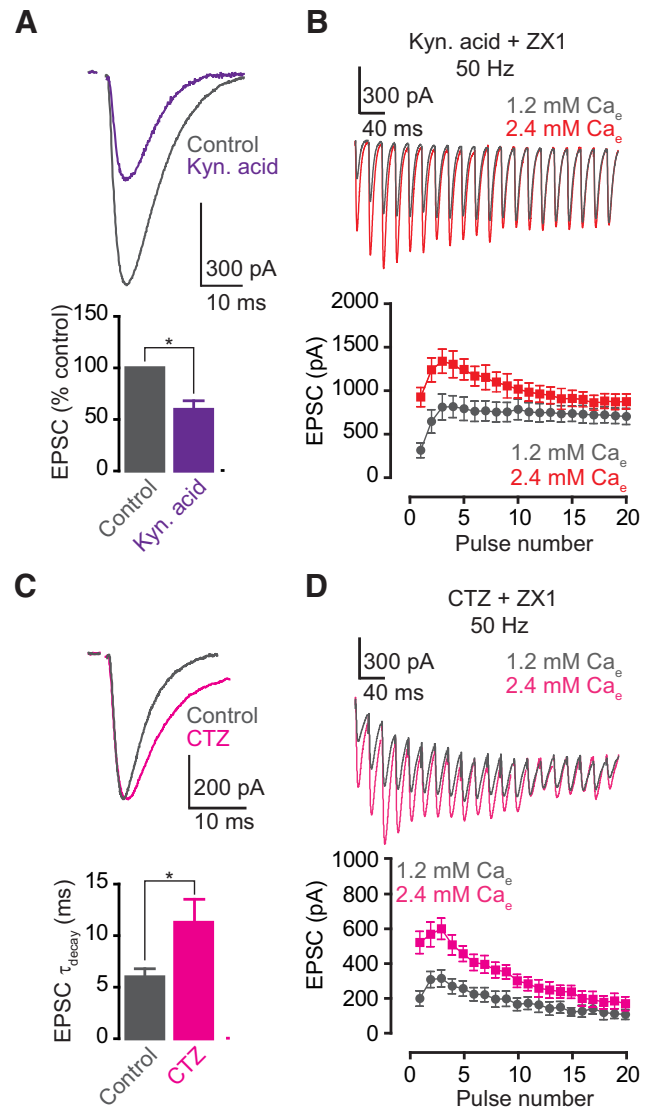


Figure 4. AMPAR saturation or desensitization do not contribute to the zinc-mediated enhancement of EPSC_{SS}. **A, C**, Upper panels, representative traces of AMPA EPSCs before (gray) and after (color) bath application of 0.5–1 mM kynurenic acid (**A**) and 100 μM cyclothiazide (**C**). Lower panels, summary graphs showing normalized AMPA EPSC amplitude (**A**) and decay time constant (**C**), before (gray) and after (color) 0.5–1 mM kynurenic acid (**A**) and 100 μM cyclothiazide (**C**; AMPA EPSC amplitude: control vs. kynurenic acid, *n* = 5, *p* < 0.01; AMPA EPSC decay time constant: control vs. cyclothiazide, *n* = 5, *p* = 0.04). **B, D**, Upper panels, representative traces of AMPA EPSCs evoked by 50-Hz 20-pulse train in 1.2 mM (gray) and 2.4 mM (color) external calcium, in 0.5–1 mM kynurenic acid and ZX1 (**B**) or in 100 μM cyclothiazide and ZX1 (**D**). Lower panels, summary graphs showing average AMPA EPSC amplitudes during the train, in kynurenic acid and ZX1 (**B**), or in cyclothiazide and ZX1 (**D**). (EPSC_{16–20} amplitude: kynurenic acid: 1.2 vs. 2.4 mM calcium, *n* = 5, *p* = 0.13; cyclothiazide: 1.2 vs. 2.4 mM calcium, *n* = 5, *p* = 0.06.) Values represent mean ± SEM. Detailed values and statistical tests: **A**, lower panel: AMPA EPSC amplitude in the presence of kynurenic acid: 59.63% ± 8.5% of baseline, *n* = 5, *p* < 0.01, *t* = 4.74, *df* = 4; one-sample *t*-test. **C**, lower panel: AMPA EPSC decay time constant: control vs. cyclothiazide: 5.99 ± 0.81 vs. 11.32 ± 2.15, *n* = 5, *p* = 0.04; paired

continued

t-test, $t = 2.95$, $df = 4$. **B**, lower panel: EPSC_{16–20} amplitude: kynurenic acid: 1.2 mM calcium: 718 pA \pm 94 pA vs. 2.4 mM calcium: 812 pA \pm 96 pA, $n = 5$, $p = 0.13$, $F = 2.37$, $DFn = 1$, $DFd = 40$; two-way ANOVA. **D**, lower panel: cyclothiazide: 1.2 mM calcium: 122 pA \pm 32 pA vs. 2.4 mM calcium: 186 pA \pm 41 pA, $n = 5$, $p = 0.06$, $F = 3.6$, $DFn = 1$, $DFd = 40$; two-way ANOVA.

contrast, in the presence of AM-251, ZX1 did not decrease AMPA EPSC facilitation (Fig. 5B), suggesting that endocannabinoid signaling and enhanced synaptic facilitation are necessary for the zinc-mediated augmentation of EPSC_{SS}.

Consistent with the lack of effect of ZX1 in enhancing EPSC_{SS} at lower stimulation frequencies (Fig. 1A, B, D, E), ZX1 did not affect synaptic facilitation at these frequencies in either 1.2 or 2.4 mM Ca_e (Fig. 6A–D). In contrast, ZX1 decreased synaptic facilitation at 50 Hz in 1.2 mM Ca_e. However, ZX1 decreased synaptic facilitation by the eighth pulse in 1.2 mM Ca_e, but in 2.4 mM Ca_e it decreased facilitation by the third pulse (Fig. 5A vs. Fig. 6E). This

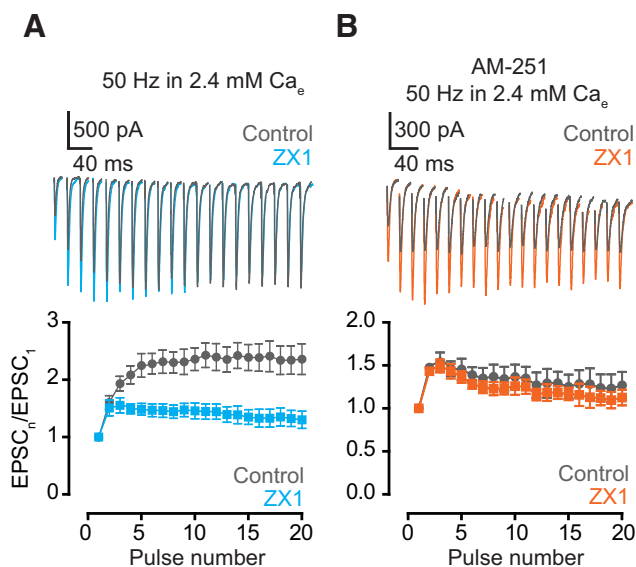


Figure 5. Enhanced zinc-mediated synaptic facilitation depends on endocannabinoid signaling. **A**, **B**, Upper panels, representative traces of AMPA EPSCs evoked by 50-Hz 20-pulse train before (gray) and after ZX1 application (color), in the absence (**A**) or presence (**B**) of AM-251. Lower panels, summary graphs showing average AMPA EPSC amplitudes during the train, normalized to EPSC amplitude elicited by first pulse, before (**A** and **B**, gray) and after (**A** and **B**, color) ZX1 application, in the absence (**A**), or presence (**B**) of AM-251 (ratio of the amplitude of 16–20 EPSC to first EPSC at 50 Hz: in the absence of AM-251: control vs. ZX1, $n = 10$, $p < 0.01$; in the presence of AM-251: control vs. ZX1, $n = 5$, $p = 0.32$). Values represent mean \pm SEM. Detailed values and statistical tests: Lower panels: ratio of the amplitude of 16–20 EPSC to first EPSC at 50 Hz: in the absence of AM-251: control: 2.29 ± 0.25 vs. ZX1: 1.32 ± 0.15 , $n = 10$, $p < 0.01$, $F = 52.81$, $DFn = 1$, $DFd = 90$; in the presence of AM-251: control: 1.19 ± 0.15 vs. ZX1: 1.04 ± 0.09 , $n = 5$, $p = 0.32$, $F = 1.0$, $DFn = 1$, $DFd = 40$; two-way ANOVA.

result is consistent with the more robust zinc-dependent endocannabinoid signaling occurring at higher Pr, which is reflected by the requirement for fewer stimuli to elicit endocannabinoid release in higher Pr (Perez-Rosello et al., 2013). Finally, ZX1 did not change synaptic facilitation at 50 Hz in ZnT3KO mice (Fig. 6F–H). Together, these results suggest that synaptically released zinc results in increased synaptic facilitation and enhanced EPSC_{SS}, via retrograde endocannabinoid signaling and decreased Pr.

Elimination of the postsynaptic inhibitory effect of zinc on AMPA EPSC amplitude during the 50-Hz train could also contribute to the zinc-mediated enhancement of synaptic facilitation. To explore this possibility, we occluded the endocannabinoid-mediated effect on synaptic facilitation by applying 50 nM WIN 55, 212-2 (WIN), a CB1 receptor activator. Then, we tested whether this occlusion affected the ZX1 potentiation of the EPSC throughout the train. If a potential reduction of the postsynaptic inhibitory effect of zinc on AMPA EPSC amplitude during the 50-Hz train was contributing to the zinc-mediated enhancement of synaptic facilitation, then occlusion of synaptic facilitation with WIN would also show a gradual reduction in the ZX1 potentiation throughout the train, as in Fig. 1D. We found that WIN occluded the effect of ZX1 on synaptic facilitation (Fig. 7A, B), and there was no reduction in the amount of ZX1 potentiation throughout the 50-Hz train (Fig. 7A, C). This result suggests that changes in the magnitude of the postsynaptic inhibitory effect of zinc on AMPA EPSC do not contribute to the zinc-mediated enhancement of synaptic facilitation.

Discussion

Our results indicate that the effects of synaptically released zinc on excitatory neurotransmission are not purely inhibitory as previously thought, for zinc's actions depend on the level of activity of the target synapses. For synapses that are active at high rates of presynaptic activity, synaptically released zinc leads to an initial inhibition of postsynaptic activity, likely via direct inhibition of AMPARs (Kalappa et al., 2015), followed by the recruitment of endocannabinoid signaling that leads to reduced Pr but enhanced steady-state EPSCs. This seemingly paradoxical effect is likely explained by the fact that increased Pr depletes presynaptic vesicles, saturates release, and limits the extent of facilitation (Zucker and Regehr, 2002; Jackman et al., 2016). Whereas our findings are consistent with this hypothesis, we cannot rule out potential effects of presynaptic endocannabinoid signaling on the presynaptic calcium signal that induces facilitation or on the calcium sensor synaptotagmin 7, which is required for synaptic facilitation (Jackman et al., 2016).

Facilitating synapses favor the transmission of burst-like presynaptic stimuli (Lisman, 1997; Abbott and Regehr, 2004). Whereas *in vivo* recordings from DCN granule cells have not been obtained, sensory stimulation produces bursts of high-frequency (>200 Hz) spikes in cerebellar granule cells (Chadderton et al., 2004). Although these bursts are briefer than the trains we used here, they also occur at higher frequencies. Based on our results

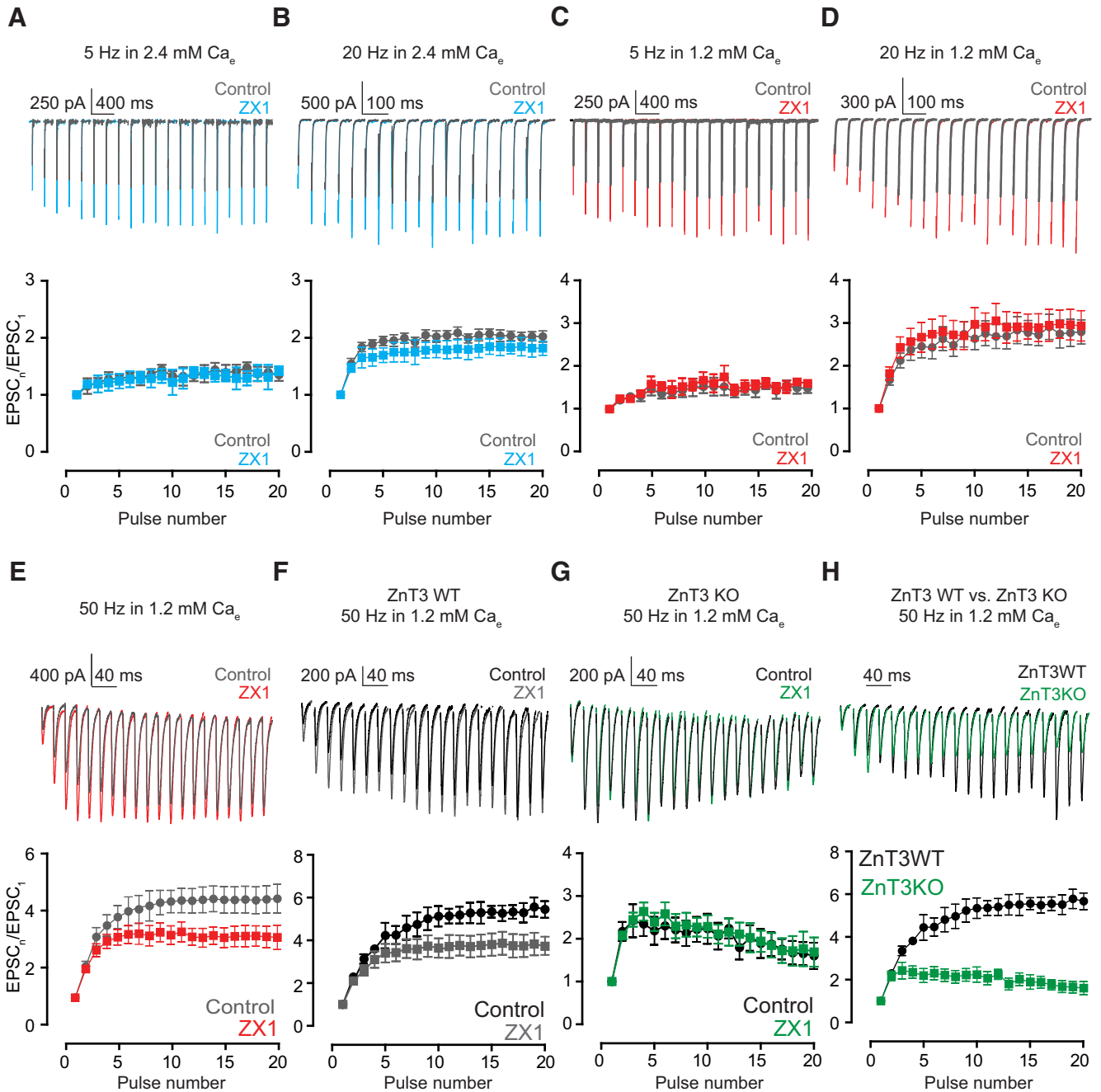


Figure 6. AMPA EPSC facilitation by synaptically released zinc is frequency, history, and Pr dependent. **A, B**, Upper panels, representative traces of AMPA EPSCs evoked by 20-pulse train at 5 Hz (**A**) and 20 Hz (**B**), before (gray) and after (color) 100 μM ZX1, in 2.4 mM external calcium. Lower panels, summary graphs showing average AMPA EPSC amplitudes during the 20-pulse train, normalized to EPSC amplitude of the first pulse, before (gray) and after (color) ZX1 application at 5 Hz (**A**) and 20 Hz (**B**), in 2.4 mM external calcium (ratio of the amplitude of 16–20 EPSC to first EPSC: 2.4 mM calcium: 5 Hz: control vs. ZX1, n = 5, p = 0.58; 20 Hz: control vs. ZX1, n = 5, p = 0.09). **C–E**, Upper panels, representative traces of AMPA EPSCs evoked by 20-pulse train at 5 Hz (**C**), 20 Hz (**D**), and 50 Hz (**E**), before (gray) and after (color) 100 μM ZX1, in 1.2 mM external calcium. Lower panels, summary graphs showing average AMPA EPSC amplitudes during the 20-pulse train, normalized to EPSC amplitude of the first pulse, before (gray) and after (color) ZX1 application at 5 Hz (**C**), 20 Hz (**D**), and 50 Hz (**E**) in 1.2 mM external calcium (ratio of the amplitude of 16–20 EPSC to first EPSC: 1.2 mM calcium: 5 Hz: control vs. ZX1, n = 5, p = 0.34; 20 Hz: control vs. ZX1, n = 5, p = 0.45; 50 Hz vs. ZX1, n = 10, p < 0.01). **F, G**, Upper panels, representative traces of AMPA EPSCs evoked by 50-Hz 20-pulse train, before (black) and after (color) 100 μM ZX1, in ZnT3WT (**F**) and ZnT3KO (**G**) mice. Lower panels, summary graphs showing average AMPA EPSC amplitudes during the 50-Hz 20-pulse train, normalized to EPSC amplitude of the first pulse, before (black) and after (color) ZX1 application, in ZnT3WT (**F**) and ZnT3KO (**G**) mice (ratio of the amplitude of 16–20 EPSC to first EPSC: ZnT3WT mice: 50 Hz: control vs. ZX1, n = 6, p < 0.01; ZnT3KO mice: 50 Hz: control vs. ZX1, n = 5, p = 0.85). **H**, Upper panel, representative traces of peak-scaled AMPA EPSCs evoked by 50-Hz 20-pulse train in ZnT3WT (black) and ZnT3KO mice (green). Lower panel, summary graphs showing average AMPA

continued

EPSC amplitudes during the 50-Hz 20 pulse train, normalized to EPSC amplitude of the first pulse in control conditions, in ZnT3WT (black) and ZnT3KO (color) mice (ratio of the amplitude of 20 EPSC to first EPSC: ZnT3WT vs. ZnT3KO: control: 50 Hz, $n = 5$, $p < 0.01$). Values represent mean \pm SEM.

Detailed values and statistical tests: **A, B**, lower panels: ratio of the amplitude of 16–20 EPSC to first EPSC: 2.4 mM calcium: 5 Hz: control: 1.40 ± 0.12 vs. ZX1: 1.34 ± 0.15 , $n = 5$, $p = 0.58$, $F = 0.31$, $DFn = 1$, $DFd = 40$; 20 Hz: control: 2.03 ± 0.09 vs. ZX1: 1.83 ± 0.14 , $n = 5$, $p = 0.09$, $F = 3.0$, $DFn = 1$, $DFd = 40$; two-way ANOVA. **C–E**, lower panels: ratio of the amplitude of 16–20 EPSC to first EPSC: 1.2 mM calcium: 5 Hz: control: 1.54 ± 0.14 vs. ZX1: 1.61 ± 0.11 , $n = 5$, $p = 0.34$, $F = 0.9$, $DFn = 1$, $DFd = 40$; 20 Hz: control: 2.78 ± 0.29 vs. ZX1: 2.94 ± 0.34 , $n = 5$, $p = 0.45$, $F = 0.56$, $DFn = 1$, $DFd = 40$; 50 Hz: 4.44 ± 0.47 vs. ZX1: 3.14 ± 0.37 , $n = 10$, $p < 0.01$, $F = 22.59$, $DFn = 1$, $DFd = 90$; two-way ANOVA. **F, G**, lower panels: ratio of the amplitude of 16–20 EPSC to first EPSC: ZnT3WT mice: 50 Hz: 5.580 ± 0.39 vs. ZX1: 3.96 ± 0.55 , $n = 6$, $p < 0.01$, $F = 28.37$, $DFn = 1$, $DFd = 50$; ZnT3KO mice: control: 50 Hz: 1.71 ± 0.27 vs. ZX1: 1.74 ± 0.33 , $n = 5$, $p = 0.85$, $F = 0.04$, $DFn = 1$, $DFd = 40$; two-way ANOVA. **H**, lower panel: ratio of the amplitude of 16–20 EPSC to first EPSC: ZnT3WT vs. ZnT3KO: control: 50 Hz: 5.58 ± 0.39 vs. 1.71 ± 0.27 , $n = 5$, $p < 0.01$, $t = 8.15$, $df = 8$; unpaired t -test.

showing that fewer stimuli are needed to elicit endocannabinoid signaling during higher stimulation frequencies (compare Fig. 5A and Fig. 6E), we expect that higher stimulation frequencies would also require fewer stimuli for eliciting the enhancing effect of zinc on steady-state EPSCs. Therefore, given the strong resemblance between DCN and cerebellar granule cells (Oertel and Young, 2004), we hypothesize that the effect of zinc in maintaining enhanced synaptic facilitation during bursts of activity may enhance information flow in cartwheel cells. However, because our *in vitro* stimulation may be stronger than the *in vivo* pattern of activity, further *in vivo* studies using natural stimuli are required to determine how synaptic zinc affects information coding in the molecular layer of the DCN.

We previously reported that synaptically released zinc decreases post-tetanic potentiation induced by high-frequency stimulation (Perez-Rosello et al., 2013); how-

ever, the effect of zinc during the high-frequency stimulation had not been studied. By assessing the role of synaptically released zinc during low- and high-frequency trains, we found that synaptic strength at intensely active synapses is larger under conditions that inhibit Pr, such as zinc-dependent endocannabinoid signaling. These results complement and extend previous studies on presynaptic GABA_B receptors, which sustain neurotransmission at higher stimulus frequencies by reducing Pr and, in turn, controlling AMPAR desensitization (Brenowitz et al., 1998; Brenowitz and Trussell, 2001). Whereas zinc and GABA_B receptors exert their context-dependent effects via different mechanisms, a common concept emerges supporting that neuromodulatory systems that combine pre- and postsynaptic mechanisms of actions also display a unique flexibility in mediating bidirectional modulation of EPSC strength (Tzounopoulos et al., 2007).

Our findings on zinc-mediated promotion of endocannabinoid signaling are consistent with our previous report showing that during high-frequency stimulation synaptic zinc release, activation of GPR39 receptors and subsequent rises in postsynaptic calcium and phospholipase C activation are necessary for triggering the synthesis of the endocannabinoid 2-arachidonoylglycerol in PF DCN synapses (Perez-Rosello et al., 2013). Moreover, the lack of zinc-dependent enhancement in EPSC_{SS} during lower stimulation frequencies, as well as the development of the endocannabinoid-mediated effect later in the train during high-frequency stimulation, are consistent with the notion that endocannabinoid signaling in DCN synapses is recruited in response to sustained high-frequency bursts of neuronal activity (Sedlacek et al., 2011; Perez-Rosello et al., 2013).

Prior studies have reported a lack of effect of synaptic zinc on short-term synaptic plasticity of AMPA EPSCs in zinc-rich hippocampal mossy fiber to CA3 (MF-CA3) or Schaffer collateral to CA1 (SC-CA1) synapses (Vogt et al., 2000; Vergnano et al., 2014). The lack of effect in these studies could be because the investigated synapses lack or express weak endocannabinoid signaling (Ohno-Shosaku et al., 2002; Hofmann et al., 2008). Moreover, these studies used a narrower range of stimulation frequencies that did not exceed 25 Hz. This could also explain the lack of effect of zinc on short-term plasticity, because higher or more sustained stimulation frequencies

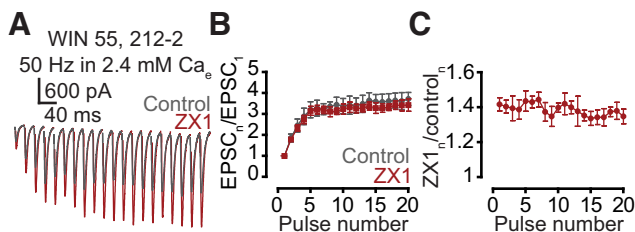


Figure 7. The postsynaptic inhibitory effect of zinc on AMPA EPSC does not contribute to the zinc-mediated enhancement of synaptic facilitation. **A**, Representative traces of AMPA EPSCs, evoked by 50-Hz 20-pulse train in the presence of 50 nM WIN 55 212-2, before (gray) and after (maroon) ZX1. **B**, Summary graph showing average AMPA EPSC amplitudes during the train, normalized to EPSC amplitude elicited by the first pulse, before (gray) and after (maroon) ZX1 (ratio of the amplitude of 16–20 EPSC to first EPSC at 50 Hz: control vs. ZX1, $n = 5$, $p = 0.18$). **C**, Summary graph showing average ratios of AMPA EPSCs in the presence of ZX1 to that in control during the train ($ZX_{1-2}/control_{1-2}$ vs. $ZX_{16-20}/control_{16-20}$, $n = 5$, $p = 0.23$). Values represent mean \pm SEM.

Detailed values and statistical tests: **B**, Ratio of the amplitude of 16–20 EPSC to first EPSC at 50 Hz: control: 3.63 ± 0.35 vs. ZX1: 3.23 ± 0.22 , $n = 5$, $p = 0.18$, $F = 1.84$, $DFn = 1$, $DFd = 40$; two-way ANOVA; **C**, $ZX_{1-2}/control_{1-2}$ vs. $ZX_{16-20}/control_{16-20}$: 1.40 ± 0.04 vs. 1.35 ± 0.05 , $n = 5$, $p = 0.23$, $t = 1.39$, $df = 4$, paired t -test.

are required for the recruitment of endocannabinoid signaling (Perez-Rosello et al., 2013), which, in turn, is crucial for the effects of zinc on short-term plasticity of glutamatergic neurotransmission. Finally, although these studies used ZnT3KO mice to eliminate synaptic zinc, zinc was chelated with tricine or CaEDTA. However, CaEDTA has slower kinetics for zinc binding than ZX1, and tricine has weaker zinc-binding affinity than ZX1 (Anderson et al., 2015). Therefore, CaEDTA and tricine are less efficient than ZX1 for investigating the effects of fast, transient elevations of synaptic zinc on synaptic targets, such as NMDAR and AMPARs (Anderson et al., 2015; Kalappa et al., 2015). Together, these data suggest that the context-dependent effect of zinc on glutamatergic neurotransmission is synapse specific and, like the effects of other neuromodulatory systems, depends on the molecular composition, structure, and function of different synapses.

Recent studies explored the dynamics of zinc in the synaptic cleft and extracellular space (Vergnano et al., 2014; Anderson et al., 2015), but less is known about the presynaptic zinc dynamics. Whereas one study suggests that zinc-containing vesicles predominantly dominate the reserve pool of synaptic vesicles (Lavoie et al., 2011), the exocytosis and endocytosis dynamics of zinc-containing vesicles remain unknown. Our results are inconsistent with depletion of zinc-containing vesicles during the high-frequency train, for ZX1 revealed no change in the amount of AMPA EPSC potentiation throughout the train of stimuli in the presence of exogenously applied cannabinoids (Fig. 7). This conclusion is based on the assumption that zinc-mediated AMPA EPSC inhibition tracks synaptic zinc levels in the cleft. However, recent results proposed AMPA EPSC modulation via intracellular zinc signaling in cultured hippocampal neurons (Arons et al., 2016). As such, transient increases in extracellular zinc after synaptic stimulation could lead to translocation of zinc into the postsynaptic neuron via zinc-permeable AMPARs (Jia et al., 2002), inducing, in turn, changes in intracellular zinc levels and modulation of AMPA EPSCs that does not track extracellular zinc levels. NMDARs contain extracellular high-affinity binding sites capable of tracking extracellular zinc levels (Paoletti et al., 2009; Hansen et al., 2014), and therefore future studies assessing the effect of synaptic zinc on NMDARs, or using localized extracellular zinc-sensitive dyes to quantify zinc levels during trains of presynaptic activity, are needed for elucidating the time course of exocytosis and endocytosis of zinc-containing vesicles.

In summary, this work demonstrates that during high-frequency trains of presynaptic activity, synaptic zinc scales glutamatergic neurotransmission bidirectionally. During the onset of activity, glutamatergic neurotransmission is scaled down predominantly by postsynaptic zinc inhibition; however, later in the train, zinc-dependent endocannabinoid signaling decreases Pr, which, in turn, increases synaptic facilitation. This enhancement overrides the Pr decrease and postsynaptic zinc inhibitory effects, thus resulting in overall enhanced synaptic strength.

References

- Abbott LF, Regehr WG (2004) Synaptic computation. *Nature* 431, 796–803. [CrossRef Medline](#)
- Anderson CT, Radford RJ, Zastrow ML, Zhang DY, Apfel UP, Lippard SJ, Tzounopoulos T (2015) Modulation of extrasynaptic NMDA receptors by synaptic and tonic zinc. *Proc Natl Acad Sci U S A* 112, E2705–E2714. [CrossRef Medline](#)
- Arons MH, Lee K, Thynne CJ, Kim SA, Schob C, Kindler S, Montgomery JM, Garner CC (2016) Shank3 is part of a zinc-sensitive signaling system that regulates excitatory synaptic strength. *J Neurosci* 36, 9124–9134. [CrossRef](#)
- Brenowitz S, David J, Trussell L (1998) Enhancement of synaptic efficacy by presynaptic GABA(B) receptors. *Neuron* 20, 135–141. [Medline](#)
- Brenowitz S, Trussell LO (2001) Minimizing synaptic depression by control of release probability. *J Neurosci* 21, 1857–1867. [Medline](#)
- Chadderton P, Margrie TW, Häusser M (2004) Integration of quanta in cerebellar granule cells during sensory processing. *Nature* 428, 856–860. [CrossRef Medline](#)
- Chen C, Blitz DM, Regehr WG (2002) Contributions of receptor desensitization and saturation to plasticity at the retinogeniculate synapse. *Neuron* 33, 779–788. [Medline](#)
- Cole TB, Wenzel HJ, Kafer KE, Schwartzkroin PA, Palmiter RD (1999) Elimination of zinc from synaptic vesicles in the intact mouse brain by disruption of the ZnT3 gene. *Proc Natl Acad Sci U S A*, 96, 1716–1721. [CrossRef](#)
- Foster KA, Kreitzer AC, Regehr WG (2002) Interaction of postsynaptic receptor saturation with presynaptic mechanisms produces a reliable synapse. *Neuron* 36, 1115–1126. [CrossRef](#)
- Frederickson CJ, Howell GA, Haigh MD, Danscher G (1988) Zinc-containing fiber systems in the cochlear nuclei of the rat and mouse. *Hear Res* 36, 203–211. [CrossRef](#)
- Frederickson CJ, Koh JY, Bush AI (2005) The neurobiology of zinc in health and disease. *Nature Rev Neurosci* 6, 449–462. [CrossRef Medline](#)
- Hansen KB, Ogden KK, Yuan H, Traynelis SF (2014) Distinct functional and pharmacological properties of triheteromeric GluN1/GluN2A/GluN2B NMDA receptors. *Neuron* 81, 1084–1096. [CrossRef Medline](#)
- Hofmann ME, Nahir B, Frazier CJ (2008) Excitatory afferents to CA3 pyramidal cells display differential sensitivity to CB1 dependent inhibition of synaptic transmission. *Neuropharmacology* 55, 1140–1146. [CrossRef](#)
- Jackman SL, Turecek J, Belinsky JE, Regehr WG (2016) The calcium sensor synaptotagmin 7 is required for synaptic facilitation. *Nature* 529, 88–91. [CrossRef Medline](#)
- Jia Y, Jeng JM, Sensi SL, Weiss JH (2002) Zn²⁺ currents are mediated by calcium-permeable AMPA/kainate channels in cultured murine hippocampal neurones. *J Physiol* 543, 35–48. [CrossRef](#)
- Kalappa BI, Anderson CT, Goldberg JM, Lippard SJ, Tzounopoulos T (2015) AMPA receptor inhibition by synaptically released zinc. *Proc Natl Acad Sci U S A* 112, 15749–15754. [CrossRef Medline](#)
- Kelleher SL, McCormick NH, Velasquez V, Lopez V (2011) Zinc in specialized secretory tissues: roles in the pancreas, prostate, and mammary gland. *Adv Nutr* 2, 101–111. [CrossRef](#)
- Kreitzer AC, Regehr WG (2000) Modulation of transmission during trains at a cerebellar synapse. *J Neurosci* 20, 1348–1357. [Medline](#)
- Kreitzer AC, Regehr WG (2002) Retrograde signaling by endocannabinoids. *Curr Opin Neurobiol* 12, 324–330. [Medline](#)
- Lan R, Liu Q, Fan P, Lin S, Fernando SR, McCallion D, Pertwee R, Makriyannis A (1999) Structure-activity relationships of pyrazole derivatives as cannabinoid receptor antagonists. *J Med Chem* 42, 769–776. [CrossRef](#)
- Lavoie N, Jeyaraju DV, Peralta MR 3rd, Seress L, Pellegrini L, Toth K (2011) Vesicular zinc regulates the Ca²⁺ sensitivity of a subpopulation of presynaptic vesicles at hippocampal mossy fiber terminals. *J Neurosci* 31, 18251–18265. [CrossRef](#)

- Lisman JE (1997) Bursts as a unit of neural information: making unreliable synapses reliable. *Trends Neurosci* 20, 38–43. [CrossRef](#) [Medline](#)
- Manis PB, Spirou GA, Wright DD, Paydar S, Ryugo DK (1994) Physiology and morphology of complex spiking neurons in the guinea pig dorsal cochlear nucleus. *J Compar Neurol* 348, 261–276. [CrossRef](#)
- Neher E, Sakaba T (2001) Combining deconvolution and noise analysis for the estimation of transmitter release rates at the calyx of held. *J Neurosci* 21, 444–461. [Medline](#)
- Oertel D, Young ED (2004) What's a cerebellar circuit doing in the auditory system? *Trends Neurosci* 27, 104–110. [CrossRef](#) [Medline](#)
- Ohno-Shosaku T, Tsubokawa H, Mizushima I, Yoneda N, Zimmer A, Kano M (2002) Presynaptic cannabinoid sensitivity is a major determinant of depolarization-induced retrograde suppression at hippocampal synapses. *J Neurosci* 22, 3864–3872.
- Pan E, Zhang XA, Huang Z, Krezel A, Zhao M, Tinberg CE, Lippard SJ, McNamara JO (2011) Vesicular zinc promotes presynaptic and inhibits postsynaptic long-term potentiation of mossy fiber-CA3 synapse. *Neuron* 71, 1116–1126. [CrossRef](#)
- Paoletti P, Vergnano AM, Barbour B, Casado M (2009) Zinc at glutamatergic synapses. *Neuroscience* 158, 126–136. [CrossRef](#) [Medline](#)
- Partin KM, Fleck MW, Mayer ML (1996) AMPA receptor flip/flop mutants affecting deactivation, desensitization, and modulation by cyclothiazide, aniracetam, and thiocyanate. *J Neurosci* 16, 6634–6647.
- Partin KM, Patneau DK, Mayer ML (1994) Cyclothiazide differentially modulates desensitization of alpha-amino-3-hydroxy-5-methyl-4-isoxazolepropionic acid receptor splice variants. *Mol Pharmacol* 46, 129–138.
- Perez-Rosello T, Anderson CT, Schopfer FJ, Zhao Y, Gilad D, Salvatore SR, Freeman BA, Hershfinkel M, Aizenman E, Tzounopoulos T (2013) Synaptic Zn²⁺ inhibits neurotransmitter release by promoting endocannabinoid synthesis. *J Neurosci* 33, 9259–9272. [CrossRef](#)
- Prescott C, Weeks AM, Staley KJ, Partin KM (2006) Kynurenic acid has a dual action on AMPA receptor responses. *Neurosci Lett* 402, 108–112. [CrossRef](#) [Medline](#)
- Sedlacek M, Tipton PW, Brenowitz SD (2011) Sustained firing of cartwheel cells in the dorsal cochlear nucleus evokes endocannabinoid release and retrograde suppression of parallel fiber synapses. *J Neurosci* 31, 15807–15817. [CrossRef](#)
- Sindreu CB, Varoqui H, Erickson JD, Pérez-Clausell J (2003) Boutons containing vesicular zinc define a subpopulation of synapses with low AMPAR content in rat hippocampus. *Cereb Cortex* 13, 823–829. [Medline](#)
- Trussell LO, Zhang S, Raman IM (1993) Desensitization of AMPA receptors upon multiquantal neurotransmitter release. *Neuron* 10, 1185–1196. [Medline](#)
- Tzounopoulos T, Kim Y, Oertel D, Trussell LO (2004) Cell-specific, spike timing-dependent plasticities in the dorsal cochlear nucleus. *Nature Neurosci* 7, 719–725. [CrossRef](#)
- Tzounopoulos T, Rubio ME, Keen JE, Trussell LO (2007) Coactivation of pre- and postsynaptic signaling mechanisms determines cell-specific spike-timing-dependent plasticity. *Neuron* 54, 291–301. [CrossRef](#)
- Vallee BL (1988) Zinc: biochemistry, physiology, toxicology and clinical pathology. *Biofactors* 1, 31–36. [Medline](#)
- Vergnano AM, Rebola N, Savtchenko LP, Pinheiro PS, Casado M, Kieffer BL, Rusakov DA, Mülle C, Paoletti P (2014) Zinc dynamics and action at excitatory synapses. *Neuron* 82, 1101–1114. [CrossRef](#) [Medline](#)
- Vogt K, Mellor J, Tong G, Nicoll R (2000) The actions of synaptically released zinc at hippocampal mossy fiber synapses. *Neuron* 26, 187–196. [Medline](#)
- Wadiche JI, Jahr CE (2001) Multivesicular release at climbing fiber-Purkinje cell synapses. *Neuron* 32, 301–313. [Medline](#)
- Wilson RI, Nicoll RA (2002) Endocannabinoid signaling in the brain. *Science* 296, 678–682. [CrossRef](#) [Medline](#)
- Zhang S, Oertel D (1993) Cartwheel and superficial stellate cells of the dorsal cochlear nucleus of mice: intracellular recordings in slices. *J Neurophysiol* 69, 1384–1397.
- Zucker RS, Regehr WG (2002) Short-term synaptic plasticity. *Annu Rev Physiol* 64, 355–405. [CrossRef](#) [Medline](#)